Repair of Amino Acid Radicals of Apolipoprotein B100 of Low-Density Lipoproteins by Flavonoids. A Pulse Radiolysis Study with Quercetin and Rutin†

Paulo Filipe,[‡,§,||,⊥] Patrice Morlière,[§,||,⊥,@] Larry K. Patterson,[§,||] Gordon L. Hug,[||] Jean-Claude Mazière,[#] Cécile Mazière,[#] João P. Freitas,[‡] Afonso Fernandes,[‡] and René Santus*[,§,||,@]

Centro de Metabolismo e Endocrinologia da Faculdade de Medicina de Lisboa, 1649-028 Lisboa, Portugal, INSERM U.532, Institut de Recherche sur la Peau, Hôpital Saint-Louis, 1 avenue Claude Vellefaux, 75475 Paris Cedex 10, France, Radiation Laboratory, University of Notre Dame, Notre Dame, Indiana 46556, Service de Biochimie, Hôpital Nord d'Amiens, 80054 Amiens Cedex 01, France, and Laboratoire de Photobiologie, Muséum National d'Histoire Naturelle, 43 rue Cuvier, 75231 Paris Cedex 05, France

Received May 15, 2002; Revised Manuscript Received July 11, 2002

ABSTRACT: Selective oxidative damage to apolipoprotein B in LDL can be effected radiolytically by $^{\bullet}Br_2^-$ radicals. Twenty-seven Trp residues constitute major primary sites of oxidation, but two-thirds of oxidized Trps ($^{\bullet}$Trp) that are formed are repaired by intramolecular electron transfer from Tyr residues with formation of phenoxyl radicals (TyrO$^{\bullet}$). Analysis of $^{\bullet}$Trp and TyrO$^{\bullet}$ transient absorbance changes suggests that other apolipoprotein B residues, probably Cys, are oxidized. LDL-bound quercetin can efficiently repair this damage. Absorption studies show that a LDL particle has the capacity to bind ∼10 quercetin molecules through interaction with apolipoprotein B. The repair occurs by intramolecular electron transfer characterized by a rate constant of 2×10^3 s^{-1}. In contrast, rutin, a related flavonoid which does not bind to LDL, cannot repair oxidized apolipoprotein B. Urate is a hydrophilic plasma antioxidant which displays synergistic antioxidant properties with flavonoids. Urate radicals produced by $^{\bullet}Br_2^-$ can also be repaired by LDL-bound quercetin. This repair occurs with a reaction rate constant of 6.8×10^7 M^{-1} s^{-1}. Comparison with previous studies conducted with human serum albumin-bound quercetin suggests that quercetin analogues tailored to be carried preferentially by lipoproteins might be more powerful plasma antioxidants than natural quercetin carried by serum albumin.

Epidemiological studies have correlated a low incidence of cardiovascular diseases in Mediterranean cultures with diets rich in fruits and vegetables and with consumption of red wines (*1*). This protection is believed to be related to the various antioxidants found in such diets. These include not only vitamins E and C but also carotenoids and polyphenols, such as the flavonoids. Flavonoids, a group of naturally occurring benzo-γ-pyrone derivatives, are found in almost every plant, and they have long been known to be potent antioxidants (*2*, *3*). The antioxidant activity of these polyphenolic compounds has been attributed to their hydrogen donating properties which make them efficient scavengers of $^{\bullet}$OH, $O_2^{\bullet-}$, peroxyl, and alkoxyl radicals (*4*). The oxy radical scavenging capacity and hydrophobicity of the most active derivatives such as the flavone quercetin (Q)[1] have motivated numerous investigations of their ability to protect against lipid peroxidation (for a review, see ref *5*). In recent studies, we have shown that Q and rutin (R), incorporated in micelles or bound to human serum albumin, can repair the amino acid radicals $^{\bullet}$Trp and TyrO$^{\bullet}$ resulting from the one-electron oxidation of Trp and Tyr. It was demonstrated that the efficiency of and rate constant for repair of amino acid radicals by the electron transfer from Q and R strongly depend on microenvironmental factors such as electrostatic interaction, local pH, and the nature of the binding site (*6*).

Low-density lipoprotein (LDL) oxidation (*7*) is believed to be principally responsible for the pathogenesis of atherosclerosis in humans (for a review, see ref *8*). The contention that there may be a link between inhibition of lipid peroxidation by flavonoids and protection against cardiovascular diseases has, consequently, stimulated studies of the effect flavonoids may have on LDL oxidation. These studies follow the general assumption that flavonoids inhibit lipid peroxidation chain reactions induced by oxy radicals reacting with the lipid moiety of LDL (*9*). The oxidation of apoli-

† This work was supported by a travel grant from the "Museum National d'Histoire Naturelle" (L.K.P.), by Grant 347-C0 from the "Ambassade de France au Portugal" and "Instituto de Cooperação Cientifica e Tecnológica Internacional" (ICCTI), and by an INSERM-ICCTI exchange program (P.F., P.M., and R.S.). Notre Dame Radiation Laboratory is supported by the Office of Basic Energy Sciences of the U.S. Department of Energy. This is document 4378 from the Notre Dame Radiation Laboratory.

* To whom correspondence should be addressed at the Muséum National d'Histoire Naturelle. Telephone: 33-140793726. Fax: 33-140793716. E-mail: santus@mnhn.fr.

‡ Centro de Metabolismo e Endocrinologia da Faculdade de Medicina de Lisboa.

§ Muséum National d'Histoire Naturelle.

|| University of Notre Dame.

⊥ These authors contributed equally to this work.

@ Hôpital Saint-Louis.

Hôpital Nord d'Amiens.

[1] Abbreviations: Apo-B, apolipoprotein B100; HSA, human serum albumin; LDL, low-density lipoprotein; Q, quercetin; R, rutin; UH_2^-, urate.

10.1021/bi026133+ CCC: $22.00
Published on Web 08/14/2002

poprotein B100 (Apo-B) residues is thought to be a key process of atherogenesis since it has been known for a long time that modification of some of the positively charged Lys residues prevents their interaction with the finely regulated Apo-B/E receptor responsible for native LDL endocytosis (*10*). Such oxidized LDL is, in turn, recognized by the unregulated scavenger receptor of macrophages, leading to oxidized LDL accumulation and foam cell formation (*10*).

Until the beginning of the past decade, it was usually assumed that alterations of Apo-B in oxidized LDL were the consequence of lipid peroxidation. For example, the modification of Lys residues was shown to occur by reaction of their ϵ-amino groups with end products of LDL lipid peroxidation (*8*). However, in addition to its 356 Lys residues, Apo-B contains 9 free Cys, 37 Trp, and 151 Tyr residues, and it was subsequently demonstrated that residues other than Lys can be oxidized without requiring LDL lipid peroxidation. The Cys residues and the two aromatic amino acids are known to be the most oxidizable residues in other proteins (*11*), and are readily modified by various sources of oxidative and photooxidative stress (*12*−*14*). Most importantly, it was shown that oxidation of Trp residues of native LDL, induced by Cu^{2+} or by irradiation with UVB light, may initiate lipid peroxidation (*13*, *14*). It may be anticipated, therefore, that providing antioxidant protection to the most oxidizable residues of Apo-B should at least partly inhibit LDL lipid oxidation and its subsequent biological consequences. Given the peculiar role attributed to flavonoid-type antioxidants in the control of atherogenesis, we have undertaken a pulse radiolysis study of the mechanisms through which aromatic amino acid radicals of Apo-B may be formed and subsequently repaired by the flavonoids Q and R. The $^{\bullet}$Trp and TyrO$^{\bullet}$ and to a lesser extent cysteinyl (RS$^{\bullet}$) radicals have been generated in deaerated solutions of native LDL by one-electron oxidation, using the selective reactivity of $^{\bullet}Br_2^-$ radicals.

One LDL particle can tightly bind ∼10 hydrophobic Q molecules. On the other hand, no binding is observed with the more hydrophilic R molecules. It is shown that repair of long-lived amino acid radicals occurs only by electron transfer from Q, with the corresponding formation of the Q$^{\bullet}$ radical. In view of previous studies on the inhibition of LDL lipid peroxidation by flavonoids, it can be suggested that flavonoids with structural characteristics favoring binding to plasma LDL could be very effective antioxidants against oxidative modification of all LDL constituents. LDL-bound Q can also repair $^{\bullet}UH^-$ radicals produced in LDL solutions in the presence of a large excess of urate (UH_2^-), an important antioxidant that can repair $^{\bullet}$Trp and TyrO$^{\bullet}$ with the corresponding formation of the $^{\bullet}UH^-$ radical (*15*).

EXPERIMENTAL PROCEDURES

Chemicals. All chemicals were analytical grade and were used as received from the suppliers. Quercetin, rutin, Trp, and uric acid were purchased from Sigma (St. Louis, MO). The 10 mM phosphate buffer (pH 7) was prepared in pure water obtained with a reverse osmosis/deionization system from Serv-A-Pure Co. Solutions were saturated with pure N_2O.

Preparation of LDL. Lipoproteins from serum of fasting healthy human volunteers were prepared by sequential ultracentrifugation at 105000*g*. The LDL fraction was taken to be the 1.024−1.050 density fraction (*16*). This fraction, free of apolipoprotein E, was protected by 0.5 mM EDTA which was removed prior to experiments by dialysis for 24 h at 4 °C against 4 L of 10 mM phosphate buffer (pH 7) containing 0.1 M KBr. Before pulse radiolysis, dialyzed LDL solutions were diluted to a concentration of 800 nM (0.4 mg/mL) with the same buffer.

Loading LDL Solutions with Flavonoids. In the case of Q, 1% (v/v) of a 10 mM solution of Q in ethanol was added to the dialysis bag containing a stock LDL solution of ∼5 mg/mL Apo-B. The LDL solution loaded with Q was immediately transferred to the dialysis buffer at 3 °C. Because of the very low solubility of Q in the buffer, a small portion was immediately adsorbed on the dialysis bag. After overnight dialysis against 2 L of buffer, the dialysis buffer was changed and dialysis resumed for an additional 12 h. Subsequently, an LDL stock solution loaded with Q was diluted to a concentration of 800 nM, an economically acceptable concentration of 0.4 mg/mL Apo-B, and was ready for pulse radiolysis as well as for absorption spectrophotometry carried out with a UVIKON 943 spectrophotometer.

In the case of R, two procedures were used. The first one was identical to that used for Q. However, the solubility of R in buffer was high enough to allow complete removal of R from the LDL solution during dialysis. In the second procedure, no dialysis was carried out. Instead, a suspension of 200 μM R prepared in the dialysis buffer was sonicated for 2 min. Then, 5% (v/v) of this solution was added to the 800 nM LDL solution prepared for pulse radiolysis experiments.

Pulse Radiolysis. Pulse radiolysis measurements were taken with the Notre Dame Radiation Laboratory 8 MeV linear accelerator, which provides 5 ns pulses of up to 30 Gy. The principles of the detection system have been previously described (*17*, *18*). It allows one to monitor transient kinetics with a single shot on multiple time scales from 0 to 8 ms after the pulse. To avoid photolysis of LDL solutions, a Corning O-51 optical filter, which removes all wavelengths shorter than 350 nm, was placed in the analyzing light beam before the sample cell, whenever possible. Radical concentrations calculated from transient absorption data are referenced to $^{\bullet}(SCN)_2^-$ dosimetry. The extinction coefficient for $^{\bullet}(SCN)_2^-$ is taken to be 7580 ± 60 M^{-1} cm^{-1} at 472 nm, and the *G* value for $^{\bullet}$OH in an N_2O-saturated solution has been measured to be 6.13 ± 0.09 (*19*). The *G* value is the number of radicals generated per 100 eV of absorbed energy, and such numbers may be recast as radical concentrations per unit of radiation (e.g., a *G* value of 6.1 corresponds to a concentration of 0.63 μM/Gy or 0.63 μM J^{-1} kg).

To conserve costly LDL preparations, a microcell (optical path of 1 cm, volume of 120 μL) fed by 2 mm internal diameter Teflon tubing was used to record kinetics and transient spectra. Doses of ∼15−20 Gy per pulse were delivered to limit the number of shots required for adequate averaging. To avoid LDL denaturation, small volumes (25 mL) of the LDL solution were gently bubbled with pure N_2O, just prior to pulse radiolysis experiments. Where necessary for calculation, differences in radical *G* values, arising from the dependence of spur scavenging on Br^- concentration, are taken into account (*20*). Numerical integrations for

analyses of rate data were carried out using Scientist software from Micromath Scientific Software.

RESULTS AND DISCUSSION

One-Electron Oxidation of Apo-B by $^{\bullet}Br_2^-$. The one-electron oxidation of Apo-B residues was carried out according to the following reaction sequence

$$H_2O \rightsquigarrow e_{aq}, H^{\bullet}, {}^{\bullet}OH, H_2O_2$$

$$e_{aq} + N_2O \rightarrow {}^{\bullet}OH + N_2 + OH^- \quad (1)$$

$${}^{\bullet}OH + 2Br^- \rightarrow {}^{\bullet}Br_2^- + OH^- \quad (2)$$

$${}^{\bullet}Br_2^- + \text{Apo-B} + H_2O \rightarrow {}^{\bullet}\text{Apo-B} + 2Br^- + H_3O^+ \quad (3)$$

$${}^{\bullet}Br_2^- + {}^{\bullet}Br_2^- \rightarrow \text{products} \quad (4)$$

In pulse radiolysis of N_2O-saturated solutions, $^{\bullet}Br_2^-$ is produced with a yield (*G*) of 6.2. Because of its redox potential, $^{\bullet}Br_2^-$ reacts selectively with certain amino acids (*21*). At neutral pH, it oxidizes free Trp according to the reaction

$$\text{Trp} + {}^{\bullet}Br_2^- + H_2O \rightarrow {}^{\bullet}\text{Trp} + 2Br^- + H_3O^+ \quad (5)$$

with a rate constant k_5 of 8.0×10^8 M^{-1} s^{-1} (data not shown).

The Apo-B of human LDL (molecular mass of 513 000 Da) contains 4560 amino acids of which 37 Trp, 9 free Cys (*12*), 151 Tyr, 114 His, and 78 Met residues (*22*) are potential targets of the $^{\bullet}Br_2^-$ oxidation. However, at pH 7, the inherent reactivity of Trp is 4 times that of Cys, 50 times that of Tyr, and ~2 orders of magnitude greater than that of His and Met (*21*). The transient absorption spectra of proteins in the near-UV and visible regions after oxidation with $^{\bullet}Br_2^-$ at pH 7 are due to the TyrO$^{\bullet}$ and deprotonated $^{\bullet}$Trp radicals (*21*, *23*, *24*). These radicals in proteins have transient absorptions in the visible region with maxima at 410 nm ($\epsilon \sim 2700$ M^{-1} cm^{-1}) and 520 nm ($\epsilon \sim 1750$ M^{-1} cm^{-1}) for TyrO$^{\bullet}$ and $^{\bullet}$Trp, respectively (*23*). There is a negligible contribution of the TyrO$^{\bullet}$ radical absorption at 520 nm. The $^{\bullet}$Trp radical contribution at 410 nm only amounts to 280 M^{-1} cm^{-1} (*23*).

When $^{\bullet}Br_2^-$ reacts with 30 μM Trp in the free form in buffer, i.e., a concentration equal to that of the 37 Trp residues in the LDL solution, $^{\bullet}$Trp radicals characterized by their maximum absorbance at 520 nm are produced with a *G*($^{\bullet}$Trp) of 2. They decay via simple second-order recombination kinetics with a bimolecular reaction rate constant ($2k$) of 8.0×10^8 M^{-1} s^{-1}. It should be noted that a *G*($^{\bullet}$Trp) much below the potential value of 6.2 is expected at low Trp concentrations because of the important contribution of the very fast decay of $^{\bullet}Br_2^-$ (reaction 4) which under these experimental conditions occurs with a rate constant $2k_4$ of 4.3×10^9 M^{-1} s^{-1} as measured from the decay of the $^{\bullet}Br_2^-$ transient absorbance at 360 nm (data not shown; see also Figure 3b).

The time evolution of the 520 nm transient absorbance obtained by $^{\bullet}Br_2^-$ oxidation of 800 nM native LDL is shown in Figure 1a. It must be noted that at this wavelength, besides $^{\bullet}$Trp, $^{\bullet}Br_2^-$ ($\epsilon \sim 280$ M^{-1} cm^{-1}) also contributes to the transient absorbance change immediately after the radiolytic pulse. Figure 1a demonstrates that the 520 nm transient absorbance of $^{\bullet}$Trp radicals in LDL decays by complex kinetics in contrast to the behavior of these radicals in the free form (see above). The maximum transient absorbance of $^{\bullet}$Trp radicals is reached after ~100 μs. Then, a decay of a first-order nature with a rate constant of $\sim 5 \times 10^3$ s^{-1} is observed before a stable population of $^{\bullet}$Trp radicals corresponding to a *G*($^{\bullet}$Trp) of 0.5 remains after ~800 μs (see Table 1). This kinetic behavior is independent of radiolytic dose and LDL concentration (data not shown). This is consistent with the occurrence of an *intra*molecular reaction. On the basis of results obtained with many other proteins (*23*, *24*), it can be suggested that the large number of Tyr residues in LDL favors efficient electron transfer reactions from an intact Tyr residue to a $^{\bullet}$Trp radical:

$$\text{Tyr} + {}^{\bullet}\text{Trp} \rightarrow \text{TyrO}^{\bullet} + \text{Trp} \quad (6)$$

Figure 1b shows the decay of the transient absorbance at 410 nm under the same dose conditions as in Figure 1a. At this wavelength, the main component of the large transient absorbance observed immediately after the pulse is undoubtedly due to $^{\bullet}Br_2^-$ whose molar absorptivity at 410 nm is 4900 M^{-1} cm^{-1}. Thus, the transient absorbance at 410 nm within the first ~600 μs is theoretically a combination of the $^{\bullet}Br_2^-$ decay and growth of the TyrO$^{\bullet}$ radical produced

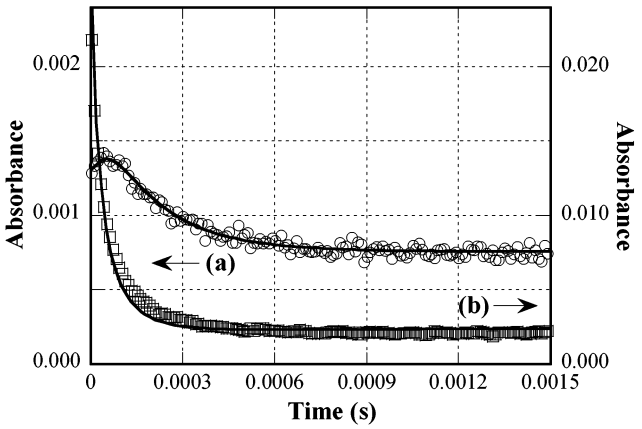

FIGURE 1: Transient absorbance changes at 520 and 410 nm. (a) Growth and decay of the transient absorption at 520 nm obtained after pulse radiolysis of an N_2O-saturated 10 mM buffered solution (pH 7) containing 100 mM KBr and 800 nM LDL. The temperature was 18 °C. The dose was 8.0 Gy. (b) Same solutions and dose conditions as in panel a but transient absorbance decay was observed at 410 nm. The solid lines show the fit of transient absorbance changes computed from rate equations 7, 9, and 11−14 (see the text).

Table 1: Radiolytic Yields of $^{\bullet}$Trp and TyrO$^{\bullet}$ Radicals after the Reaction of $^{\bullet}Br_2^-$ with LDL[a]

	G($^{\bullet}$Trp)		*G*(TyrO$^{\bullet}$)	
conditions	initial	final	initial	final
native LDL	1.5	0.5	~0	1.0
Trp alone	2[b]		na[c]	

[a] Experiments were carried out at 18 °C in 10 mM N_2O-saturated phosphate buffer (pH 7) with 100 mM Br^-. [LDL] = 800 nM, and [Trp] = 30 μM. The radiolytic dose was 8.0 Gy. [b] The *G*($^{\bullet}$Trp) in the solution containing Trp alone was measured at the maximal transient absorbance of the $^{\bullet}$Trp radicals at 520 nm (see the text). [c] Nonapplicable.

by the electron transfer to the •Trp radicals from Tyr residues and the direct reaction of Tyr residues of Apo-B with $•Br_2^-$. After this time, the remaining 410 nm transient absorption can be unequivocally attributed to the TyrO• radicals. Under the same dose conditions as in Figure 1a, G(TyrO•) measured 1.6 ms after the pulse is 1. Thus, at that time, G(•Trp) + G(TyrO•) = 1.5.

The above phenomenological study of the transient behavior and reaction sequence at 410 and 520 nm provides the basis for the determination of the kinetic parameters fully describing the oxidation of Apo-B by $•Br_2^-$. It should be noted that any pertinent set of rate equations must be able to simultaneously depict the time dependence changes of the transient absorbances at 410 and 520 nm. The following reactions are to be taken into account.

(i) The first is bimolecular decay of $•Br_2^-$ via reaction 4.

(ii) The second is selective reaction of $•Br_2^-$ with reactive residues of Apo-B, mainly Trp, Cys (RSH), and possibly Tyr and His residues via reaction 3. Lipids and antioxidants such as carotenoids, vitamin E, and retinoids whose native LDLs are natural carriers are deeply buried in the lipidic core and are thus inaccessible to reaction with $•Br_2^-$. This contention is supported by the lack of bleaching of the strong characteristic carotenoid absorbance at 450 nm during $•Br_2^-$ oxidation (data not shown). The polyunsaturated glycerophospholipids located in a monolayer at the surface of the LDL could be accessible to $•Br_2^-$. However, it has been shown that polyunsaturated fatty acids such as linolenic acid react sluggishly with $•Br_2^-$ with a rate constant of $<4 \times 10^6$ M^{-1} s^{-1} (*25*).

(iii) The third is a monomolecular electron transfer reaction from intact Tyr to part of the •Trp radicals.

Bimolecular reactions such as Apo-B + Apo-B → products can be neglected since •Trp and TyrO• are fairly stable on the time scale of Figure 1.

These complex kinetics can be explained by the following set of simultaneous rate equations:

$$d[•Br_2^-]/dt = -2k_4[•Br_2^-]^2 - k_3[\text{Apo-B}][•Br_2^-] \quad (7)$$

$$d[•Trp_R]/dt = \alpha\delta k_3[\text{Apo-B}][•Br_2^-] - k_6[•Trp_R] \quad (8)$$

$$d[•Trp_{NR}]/dt = \alpha(1-\delta)k_3[\text{Apo-B}][•Br_2^-] \quad (9)$$

$$d[\text{TyrO}•]/dt = \beta k_3[\text{Apo-B}][•Br_2^-] + k_6[•Trp_R] \quad (10)$$

$$d[X•]/dt = \gamma k_3[\text{Apo-B}][•Br_2^-] \quad (11)$$

where α, β, and γ are the proportions of $•Br_2^-$ reacting with Trp, Tyr, and other residues X of Apo-B, respectively, not absorbing light at 410 and 520 nm ($\alpha + \beta + \gamma = 1$) and where $•Trp_R$ (proportion, δ) and $•Trp_{NR}$ (proportion, $1 - \delta$) are the reparable and nonreparable •Trp radicals, respectively. Furthermore, the calculation suggests that two populations of reparable •Trp radicals are formed. The existence of concurrent reactions for the electron transfer from Tyr to •Trp radicals is well-documented in proteins with numerous Tyr and Trp residues (see several examples in ref *24*). These two independent populations of reparable •Trp radicals, $•Trp_{R1}$ and $•Trp_{R2}$ in proportions such as $[•Trp_{R1}] = \phi[•Trp_R]$ and $[•Trp_{R2}] = (1 - \phi)[•Trp_R]$, can react by *intra*molecular reaction with intact Tyr residues with rate constants $k_{6'}$ and $k_{6''}$. Hence, rate equations 8 and 10 become

$$d[•Trp_{R1}]/dt = \alpha\delta\phi k_3[\text{Apo-B}][•Br_2^-] - k_{6'}[•Trp_{R1}] \quad (12)$$

$$d[•Trp_{R2}]/dt = \alpha\delta(1-\phi)k_3[\text{Apo-B}][•Br_2^-] - k_{6''}[•Trp_{R2}] \quad (13)$$

$$d[\text{TyrO}•]/dt = \beta k_3[\text{Apo-B}][•Br_2^-] + k_{6'}[•Trp_{R1}] + k_{6''}[•Trp_{R2}] \quad (14)$$

Solving the simultaneous differential equations 7, 9, and 11−14 can be carried out knowing the initial $•Br_2^-$ concentration from dosimetry, the molar absorbances of $•Br_2^-$, •Trp, and TyrO• at 520 and 410 nm (see above), and $2k_4$ values of 4.3×10^9 M^{-1} s^{-1} from experiments performed in the absence of LDL (see above). The excellent fit of the transient absorbance at 520 nm (solid line in Figure 1a) and at 410 nm (solid line in Figure 1b) demonstrates the validity of this kinetic model. The calculation indicates negligible reactivity of $•Br_2^-$ with Tyr residues ($\beta \sim 0$), maximum reactivity with •Trp radicals ($\alpha = 0.55$), and moderate reactivity ($\gamma = 0.45$) with other Apo-B targets, most probably free Cys residues, since the latter are fairly reactive with $•Br_2^-$ (*21*). The oxidation of the numerous His residues by $•Br_2^-$ is less likely as discussed earlier in this section. The apparent reaction rate constant for the reaction of $•Br_2^-$ with Apo-B (k_3) has been determined to be 1.1×10^{10} M^{-1} s^{-1}. This apparent rate constant takes into account all possible targets and their electrostatic environment in a single molecule of Apo-B. Hence, it is much higher than that of Trp in the free form (see above).

The proportion of •Trp radicals susceptible to repair by intact Tyr is 66% (δ), of which 70% are repaired with a rate constant $k_{6'}$ of 1.5×10^4 s^{-1}, whereas the remaining 30% are repaired with a rate constant $k_{6''}$ of 5.0×10^3 s^{-1}. The nonreparable fraction of •Trp radicals represents 18% [$\alpha(1 - \delta)$] of the *overall* Apo-B damage leading to the final G(•Trp) of 0.5 given in Table 1. As a result, the initial G(•Trp) is ~1.5 since the initial G(•Trp) = G($•Trp_{NR}$) + G($•Trp_R$). Furthermore, from $\gamma = 0.45$, it can be estimated that G(Apo-B) is 1.2, leading to an overall G value for the Apo-B oxidation of 2.7. The overall value of G remains constant from the initial reaction with $•Br_2^-$, though electron transfer changes the relative contributions of G(TyrO•) and G(•Trp) to that value where G($•Trp_R$) = G(TyrO•) (see Table 1). Moreover, the comparison of the G(•Trp) of 1.5 obtained with native Apo-B to the G(•Trp) of 2 measured with Trp in the free form suggests that in native LDL, only 27 Trp residues of Apo-B are accessible to $•Br_2^-$ attack. Two-thirds of these oxidized residues can be repaired by intramolecular electron transfer from Tyr residues. This apparent oxidizability of only 8 or 9 of the 37 Trp residues of Apo-B by $•Br_2^-$ is reminiscent of the work of Giessauf et al. showing that the same number of Trp residues of Apo-B were oxidized at the initial stage of the Cu^{2+}-induced LDL oxidation (*26*). It may be thought that a similar repair of oxidized Trp by intact Tyr residues may also occur in this system.

Repair of Oxidative Damage by Quercetin and Rutin: Interaction of Quercetin and Rutin with LDL. Quercetin and

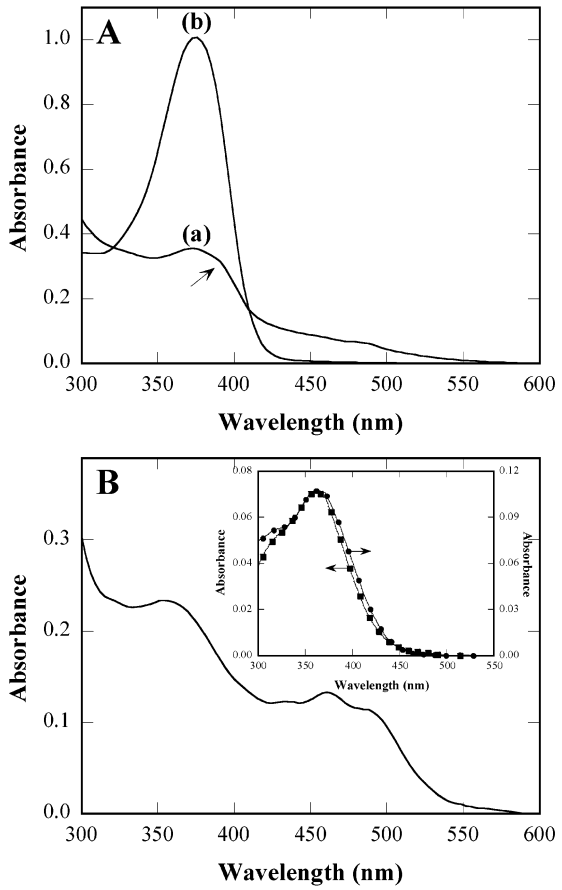

FIGURE 2: Absorption spectra of quercetin and rutin. (A) Absorption spectra of Q measured at 18 °C in 1 cm light path quartz cells. (a) Buffer (10 mM, pH 7) containing 100 mM KBr and 800 nM LDL after extensive dialysis. The arrow indicates a shoulder. (b) Ethanol with 40 μM Q. (B) Absorption spectra of 10 μM R in 10 mM buffer (pH 7) containing 100 mM KBr and 800 nM LDL measured at 18 °C in 1 cm light path quartz cells. The inset shows (●) the absorption spectrum of 10 μM R in buffer and (■) the absorption spectrum of 10 μM R in buffer in the presence of 800 nM LDL after subtraction of the absorption spectrum of the 800 nM LDL solution.

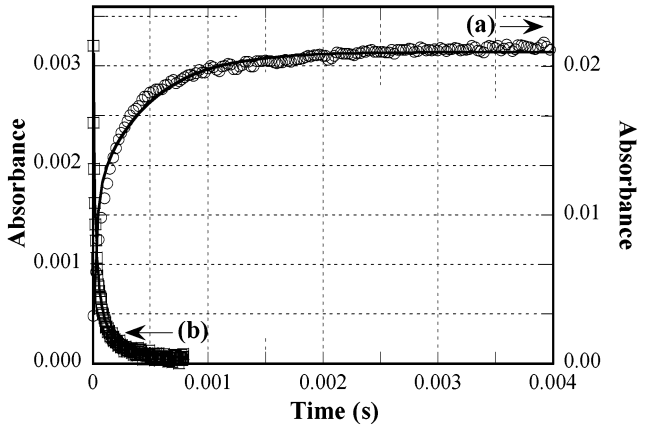

FIGURE 3: Repair of Apo-B radicals by quercetin. (a, right ordinate) Growth of the transient absorption at 620 nm obtained after pulse radiolysis of an N_2O-saturated 10 mM buffered solution (pH 7) containing 100 mM KBr and 800 nM LDL loaded with 8 μM Q. The solid line is a fit of the growth assuming a first-order process for the repair (see the text). The temperature was 18 °C. The dose was 19.8 Gy. Note an initial absorbance of ~0.0035 due to $^{\bullet}Br_2^-$ (ϵ = 260 M^{-1} cm^{-1} at 620 nm). (b, left ordinate) Decay of the transient absorption of $^{\bullet}Br_2^-$ at 620 nm in an N_2O-saturated 10 mM buffered solution (pH 7) containing 100 mM KBr. The temperature was 18 °C. The dose was 19.4 Gy.

rutin can be expected to interact with proteins because they contain hydrophobic aromatic rings and hydroxyl groups capable of hydrogen bonding with amino acid residues. For example, Q and its metabolites can bind to human serum albumin (HSA) (*27*), and the constant for the binding of Q to HSA is 2.5×10^5 (*28*). The interaction of aromatic molecules with LDL may occur through two distinct pathways. The first is simple binding of aromatic molecules to Apo-B, governed by the law of mass action in the same manner as with HSA. In addition, hydrophobic or amphiphilic molecules can be solubilized in the lipidic core of the micelle-like LDL particle where they are tightly entrapped. In this way, LDL particles constitute natural carriers of vitamin E and carotenoids. Furthermore, we have previously demonstrated that one LDL particle can incorporate more than 50 protoporphyrin or Photofrin II molecules that cannot be removed by extensive dialysis (*29*, *30*). In view of such behavior, it is necessary to know the nature of the interactions of Q and R with the LDL particle to best understand the mechanisms involved in the repair of oxidative damage to Apo-B. Figure 2A(a) demonstrates that LDL particles retain Q after extensive dialysis. The absorption spectrum of Q bound to LDL has a maximum at 375 nm corresponding to that obtained in ethanol [Figure 2A(b)] or in buffer (*27*), but the appearance of a shoulder in the Q spectrum at 390 nm, found only in the presence of an LDL solution, also suggests some interaction with hydrophobic regions of Apo-B. This contention is supported by the observation that the absorption spectrum of Q in HSA, where Q is bound to domain II A (*28*), is shifted to the red as compared to the absorption spectrum of Q in buffer (*27*). If it is assumed that the molar absorptivities of Q in ethanol and LDL are similar, it can be estimated from Figure 2A that an LDL particle has the capacity to incorporate 10 molecules of Q.

The optical absorption spectrum of R in the 800 nM LDL solution is presented in Figure 2B and does not exhibit any spectral modification when compared to that recorded in 10 mM phosphate buffer (pH 7). The inset in Figure 2B demonstrates that, after subtraction of the LDL absorption, the absorption spectrum of R in LDL solution is readily superimposed on that obtained in the absence of LDL. Furthermore, no evidence of R in the LDL solution was found after overnight dialysis of a 800 nM LDL solution loaded with 10 μM R. On the basis of these two observations, we may conclude that the interaction of R with LDL particles, if any, must be rather weak.

Repair of Oxidative Damage by Quercetin and Rutin: Kinetics of Repair of Oxidative Damage to Apo-B by Flavonoids. The repair of Apo-B damage by LDL-bound Q is illustrated in Figure 3a. This figure shows the growth of the $Q^{\bullet}$ radical measured at 620 nm after pulse radiolysis of an LDL solution loaded with 8 μM Q. The $Q^{\bullet}$ transient absorption was measured at 620 nm because it corresponds to the wavelength of the isosbestic point between the $Q^{\bullet}$ spectrum and that resulting from the subsequent transformation of $Q^{\bullet}$ radicals. The transient absorbances measured at this wavelength are, therefore, independent of the identity of the Q species absorbing at this wavelength (*6*). In an LDL solution, the formation of $Q^{\bullet}$ radicals exhibits complex

kinetics which continue throughout a time scale of several milliseconds. These processes occur long after the decay of $^{\bullet}Br_2^-$ which, in the absence of LDL, is completed after ~400 μs under similar dose conditions (Figure 3b).

We have previously demonstrated that in micellar phases or in HSA-containing solutions, Q$^{\bullet}$ is formed by electron transfer from Q to $^{\bullet}$Trp and TyrO$^{\bullet}$ radicals (*6*). Similarly, the formation of Q$^{\bullet}$ in Figure 3a can be explained at least partly by the repair of $^{\bullet}$Trp or TyrO$^{\bullet}$ radicals of Apo-B by LDL-bound Q according to *intra*molecular reactions such as

$$\text{TyrO}^{\bullet}\ (\text{or } {}^{\bullet}\text{Trp}) + \text{Q} \rightarrow \text{Tyr (or Trp)} + \text{Q}^{\bullet} \quad (15)$$

However, the radiolytic yield that can be calculated from Figure 3a 4 ms after the radiolytic pulse is 3.5, more than double that of G(TyrO$^{\bullet}$) + G($^{\bullet}$Trp). Consequently, Q$^{\bullet}$ must also be produced by other reactions. First, in addition to TyrO$^{\bullet}$ and $^{\bullet}$Trp radicals, other Apo-B residues such as the nine free Cys residues can be oxidized by $^{\bullet}Br_2^-$. At pH 7, the redox potential of the RS$^{\bullet}$,H$^+$/RSH couple is ca. 1 V. It is close to that of the $^{\bullet}$Trp,H$^+$/Trp couple and above that of the TyrO$^{\bullet}$,H$^+$/Tyr couple (*6*, *31*). As a consequence, it can be anticipated that oxidized residues other than Tyr and Trp can also be repaired by Q because of the lower redox potential of the Q$^{\bullet}$/Q couple (*32*, *33*). Both Q and R have been shown to react fairly rapidly with $^{\bullet}Br_2^-$ in micelles (*6*) or in water at pH 7 (*32*) with rate constants of $>1 \times 10^8$ M^{-1} s^{-1}. Here, the direct one-electron oxidation of Q by $^{\bullet}Br_2^-$ is likely to occur on a time scale on the order of 200 μs, corresponding roughly to the overall consumption of $^{\bullet}Br_2^-$.

The complex kinetics of Q$^{\bullet}$ growth at 620 nm have been analyzed taking into account the fact that $^{\bullet}Br_2^-$ disappears by bimolecular reaction (reaction 4) or by reacting either with residues of Apo-B (reaction 16) or with Q molecules entrapped in the LDL (reaction 17). It is assumed that all Apo-B residues oxidized by $^{\bullet}Br_2^-$ ($^{\bullet}$Apo-B,Q) undergo the electron transfer from Q (reaction 18).

$$^{\bullet}Br_2^- + \text{Apo-B,Q} \rightarrow {}^{\bullet}\text{Apo-B,Q} + 2Br^- \quad (16)$$

$$^{\bullet}Br_2^- + \text{Apo-B,Q} \rightarrow \text{Apo-B,Q}^{\bullet} + 2Br^- \quad (17)$$

$$^{\bullet}\text{Apo-B,Q} \rightarrow \text{Apo-B,Q}^{\bullet} \quad (18)$$

The rate constant k_{16} for the $^{\bullet}Br_2^-$ reaction with the Apo-B here will be essentially determined by the protein targets and thus will be the same as with Apo-B in reaction 3. It is further assumed that the electron transfer leading to Q$^{\bullet}$ formation (reaction 18) occurs by an *intra*molecular pathway with the same rate constant k_{18} for all oxidized Apo-B residues.

Hence, the above considerations allow one to write the following equations which take into account all reactions leading to the formation of Q$^{\bullet}$ radical in this system.

$$d[^{\bullet}Br_2^-]/dt = -2k_4[^{\bullet}Br_2^-]^2 - k_3[\text{Apo-B,Q}][^{\bullet}Br_2^-] - k_{17}[\text{Q}][^{\bullet}Br_2^-] \quad (19)$$

$$d[^{\bullet}\text{Apo-B,Q}]/dt = k_3[\text{Apo-B,Q}][^{\bullet}Br_2^-] - k_{18}[^{\bullet}\text{Apo-B,Q}] \quad (20)$$

$$d[\text{Apo-B,Q}^{\bullet}]/dt = k_{17}[\text{Q}][^{\bullet}Br_2^-] + k_{18}[^{\bullet}\text{Apo-B,Q}] \quad (21)$$

$$d[\text{Q}]/dt = -k_{17}[\text{Q}][^{\bullet}Br_2^-] - k_{18}[^{\bullet}\text{Apo-B,Q}] \quad (22)$$

where [Q] is the concentration of bound Q. At 620 nm, the molar extinction coefficients of $^{\bullet}Br_2^-$ and Q$^{\bullet}$ are 260 and 3200 M^{-1} cm^{-1}, respectively. Using a $2k_4$ value of 4.3×10^9 M^{-1} s^{-1}, a k_3 value of 1.1×10^{10} M^{-1} s^{-1} (see above), and the initial [$^{\bullet}Br_2^-$] from dosimetry, an excellent fit of the 620 nm growth is obtained (Figure 3b) which validates this overall kinetic model for the oxidation of Apo-B by $^{\bullet}Br_2^-$ and repair by Q. It yields the following: $k_{17} = 2.2 \times 10^9$ M^{-1} s^{-1} and $k_{18} = 2.0 \times 10^3$ s^{-1}. A rough estimate of k_{18} can be also obtained from the growth of the Q$^{\bullet}$ transient absorbance at 620 nm, measured 0.5 ms after the radiolytic pulse when all other processes have become negligible. A rate constant of $\sim 1.1 \times 10^3$ s^{-1} can be estimated, in fair agreement with the value found above.

It is interesting to compare the repair of Apo-B by bound Q to that obtained with unbound R. For this purpose, 10 μM R was added to the LDL solution instead of 8 μM Q. Comparison of trace b in Figure 3 and trace a in Figure 4 demonstrates that the small yield of R$^{\bullet}$ radical [G(R$^{\bullet}$) = 0.1] was due to its direct one-electron oxidation by $^{\bullet}Br_2^-$. Previous studies have demonstrated that HSA-bound R could repair TyrO$^{\bullet}$ and $^{\bullet}$Trp radicals produced by $^{\bullet}Br_2^-$ with the same efficiency as Q (*6*). Hence, it can be concluded that the very effective repair (close to 100%) of oxidative damage to Apo-B by Q results from its binding to LDL.

Repair of Urate Radicals by LDL-Bound Quercetin. Uric acid is an important antioxidant of plasma where it is found in its monoanionic form, UH_2^-, at a concentration of 400 μM (*32*). Because of its good electron donor properties, it repairs oxidative damage to molecules of biological interest, including amino acids. As a consequence, urate may act as an effective antioxidant to repair oxidative damage to Trp and Tyr residues in circulating proteins such as HSA (*4*). Such repair occurs with formation of the $^{\bullet}UH^-$ radicals which absorb in the near-UV region (*15*). Furthermore, an antioxidant synergy arises from the contribution of urate activity that may contribute to the beneficial effects attributed to flavonoids (*34*).

We have recently shown that the $^{\bullet}UH^-$ radical could be repaired by Q which is carried by HSA in blood and thus protected from degradation. However, the efficiency of the electron transfer from HSA-bound Q to $^{\bullet}UH^-$ is low due to the relative inaccessibility of $^{\bullet}UH^-$ radicals to domain II A of HSA where Q is bound (*6*). It is of interest to determine whether the $^{\bullet}UH^-$ radical can also be repaired by LDL-bound Q and, if so, to what extent. To this end, 100 μM urate was added to the Q-loaded LDL prior to pulse radiolysis. Under these conditions, the main radical species formed by pulse radiolysis are $^{\bullet}UH^-$ radicals since urate reacts with $^{\bullet}Br_2^-$ with a rate constant of 8.3×10^8 M^{-1} s^{-1} (*15*). The $^{\bullet}UH^-$ radicals are then repaired by electron transfer from Q solubilized in LDL, again leading to formation of Q$^{\bullet}$. Via comparison of Figure 3a and Figure 4b, it can be seen that the electron transfer from Q to $^{\bullet}UH^-$ occurs on a time scale much slower than that of the repair of Apo-B damage. In the case of urate, electron transfer involves bimolecular processes since urate radicals formed at a concentration of ~10 μM in the buffer

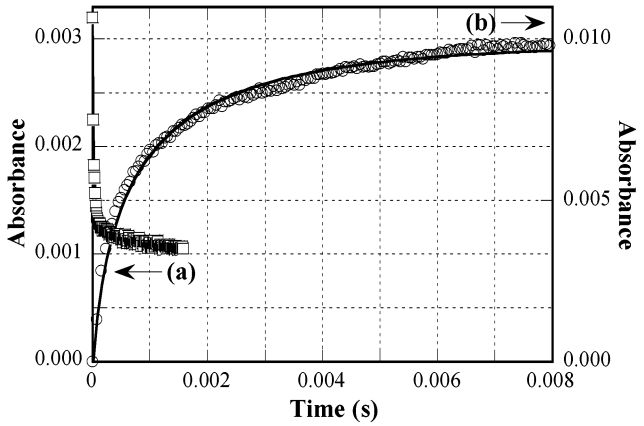

FIGURE 4: Repair of urate radicals by quercetin. (a, left ordinate) Growth and decay of the transient absorption at 620 nm obtained after pulse radiolysis of an N_2O-saturated 10 mM buffered solution (pH 7) containing 100 mM KBr and 800 nM LDL loaded with 10 μM R. The temperature was 18 °C. The dose was 19.8 Gy. (b, right ordinate) Growth of the transient absorption at 620 nm obtained after pulse radiolysis of an N_2O-saturated 10 mM buffered solution (pH 7) containing 100 mM KBr, 100 μM urate, and 800 nM LDL loaded with 8 μM Q. The solid line is a fit of the growth assuming two competitive second-order processes (see the text). The temperature was 18 °C. Note the initial absorbance due to $^{\bullet}Br_2^-$.

must encounter a Q-loaded LDL before being repaired. On the time scale that is involved, the bimolecular decay of $^{\bullet}UH^-$ radicals ($2k_{23} = 3.4 \times 10^8$ M^{-1} s^{-1}) (*15*) competes with the repair reaction (k_{24}). As a consequence, the rate equations that must be taken into account are

$$d[^{\bullet}UH^-]/dt = -2k_{23}[^{\bullet}UH^-]^2 - k_{24}[Q][^{\bullet}UH^-] \quad (23)$$

$$d[Q^{\bullet}]/dt = k_{24}[Q][^{\bullet}UH^-] \quad (24)$$

On the basis of these competitive reactions, a good fit of the calculated kinetics to the observed transient growth is readily obtained (Figure 4b), yielding a rate constant k_{24} of 6.8×10^7 M^{-1} s^{-1} for the electron transfer reaction from Q to $^{\bullet}UH^-$. In addition to these kinetic data, a yield of 1.6 can be estimated from Figure 4b for the production of $Q^{\bullet}$ radicals by the repair of urate radicals. As a consequence, the repair effectiveness of the urate oxidation by LDL-bound Q is ~25% as opposed to complete repair of Apo-B damage. The lower accessibility of $^{\bullet}UH^-$ radicals to LDL-bound Q molecules reflected by the relatively small repair rate constant added to the fast bimolecular decay of $^{\bullet}UH^-$ radicals is probably responsible for this lower effectiveness of repair. However, the rate constant for the repair of $^{\bullet}UH^-$ radicals by LDL-bound Q is ~30 times greater than that of HSA-bound Q, corresponding to a similar 30 times lower repair effectiveness of urate radicals in HSA solutions (*6*).

In conclusion, although Trp residues are the main targets of oxidation of native LDL Apo-B by $^{\bullet}Br_2^-$, a significant number of oxidized Trp residues are repaired by efficient electron transfer from intact Tyr residues. The results show that in addition to the indirect oxidation of Tyr residues by this electron transfer reaction, oxidation of other residues, presumably free Cys, contributes to the overall Apo-B damage. However, the major finding of this work is that the flavonoid Q bound to LDL can efficiently repair oxidative damage to amino acid constituents of LDL Apo-B. This is especially important since oxidation of Trp residues of Apo-B by various chemical or physical agents triggers LDL lipid peroxidation (*12*−*14*). It follows that, in addition to the well-established direct inhibition of lipid peroxidation, this protection against oxidative damage to Apo-B must contribute to the very potent antioxidant deterrent of Q to LDL oxidative modification. LDL-bound Q can also repair the radical of urate, an antioxidant which acts synergistically with Q to inhibit the Cu^{2+}-induced lipid peroxidation in plasma (*35*). In both cases, electron transfer from Q to the acceptor radical is observed. Interestingly, LDL-bound Q is a much more effective antioxidant toward amino acid radicals and urate than Q bound to HSA, its natural carrier in blood (*6*). As a consequence, it may be suggested that analogues of Q with better partitioning in blood in favor of lipoproteins combined with better mucosal absorption might afford enhanced protection against plasma lipid peroxidation and their physiological consequences.

While these studies were carried out in deaerated systems, preliminary studies with the long-lived component of $^{\bullet}$Trp in LDL indicate that these oxidized residues can also react with $O_2^{\bullet-}$ with a bimolecular rate constant of $\sim 10^8$ M^{-1} s^{-1} (data not shown), a value consistent with that found in lysozyme (*36*). As Q may also react with $O_2^{\bullet-}$ (*33*) as well as amino acid radicals, the interplay of all these species in aerated systems will determine the antioxidant capacity of Q and related flavonoids toward the protein component of LDL.

REFERENCES

1. Renaud, S., and De Lorgeril, M. (1992) *Lancet 339*, 1523−1526.
2. Harborne, J. B., Mabry, T. J., and Mabry, H. (1975) *The Flavonoids*, Chapman and Hall, London.
3. Kahl, R. (1991) Protective and adverse biological actions of phenolic antioxidants, in *Oxidative Stress. Oxidants and Antioxidants* (Sies, H., Ed.) pp 245−273, Academic Press, London.
4. Torel, J., Cillard, J., and Cillard, P. (1986) *Phytochemistry 25*, 383−385.
5. Rice-Evans, A., Miller, J., and Paganga, G. (1996) *Free Radical Biol. Med. 20*, 933−956.
6. Filipe, P., Morlière, P., Patterson, L. K., Hug, G. L., Mazière, J.-C., Mazière, C., Freitas, J. P., Fernandes, A., and Santus, R. (2002) *Biochim. Biophys. Acta 1571*, 102−114.
7. De Whalley, C., Rankin, S. M., Hoult, J. R., Jessup, W., and Leake, D. (1990) *Biochem. Pharmacol. 39*, 1743−1750.
8. Steinbrecher, U. P. (1987) *J. Biol. Chem. 262*, 3603−3608.
9. Miura, S., Watanabe, J., Sano, M., Tomita, T., Osawa, T., Hara, Y., and Tomita, I. (1995) *Biol. Pharm. Bull. 18*, 1−4.
10. Goldstein, J. L., and Brown, M. S. (1977) *Annu. Rev. Biochem. 46*, 897−930.
11. Davies, K. J. A. (1987) *J. Biol. Chem. 262*, 9895−9901.
12. Vanderyse, L., Devreese, A. M., Baert, J., Vanloo, B., Lins, L., Ruysschaert, J. M., and Rosseneu, M. (1992) *Atherosclerosis 97*, 187−199.
13. Giesauf, A., Van Wickern, B., Simat, T., Steinhart, H., and Esterbauer, H. (1996) *FEBS Lett. 389*, 136−140.
14. Salmon, S., Mazière, J.-C., Santus, R., Morlière, P., and Bouchemal, N. (1990) *Photochem. Photobiol. 52*, 541−545.
15. Santus, R., Patterson, L. K., Filipe, P., Morlière, P., Hug, G. L., Fernandes, A., and Mazière, J.-C. (2001) *Free Radical Res. 35*, 129−136.
16. Havel, J. R., Edre, H. A., and Bragdon, J. (1955) *J. Clin. Invest. 34*, 1345−1353.
17. Patterson, L. K., and Lilie, J. A. (1974) *Int. J. Radiat. Phys. Chem. 6*, 129−141.
18. Hug, G. I., Wang, Y., Schoneich, C., Jiang, P. Y., and Fessenden, R. W. (1999) *Radiat. Phys. Chem. 54*, 559−566.
19. Schuler, R. H., Patterson, L. K., and Janata, E. (1980) *J. Phys. Chem. 84*, 2088−2089.
20. La Verne, J. A., and Pimblott, S. M. (1991) *J. Phys. Chem. 95*, 3196−3206.

21. Adams, G. E. (1973) Radiation chemical mechanisms in radiation biology, in *Advances in Radiation Chemistry* (Burton, M., and Magee, J. I., Eds.) pp 146−159, John Wiley and Sons, New York.
22. Cladaras, C., Hadzopoulo-Cladaras, M., Nolte, R. T., and Zannis, V. I. (1986) *EMBO J. 5*, 3495−3507.
23. Weinstein, M., Alfassi, Z. B., Defelippis, M. R., Klapper, M. H., and Farragi, M. (1991) *Biochim. Biophys. Acta 1076*, 173−178.
24. Butler, J., Land, E. J., Prutz, W. A., and Swallow, A. J. (1982) *Biochim. Biophys. Acta 705*, 150−162.
25. Neta, P., Huie, R. E., and Ross, A. B. (1988) *J. Phys. Chem. Ref. Data 17*, 1027−1284.
26. Giessauf, A., Steiner, E., and Esterbauer, H. (1995) *Biochim. Biophys. Acta 1256*, 221−232.
27. Manach, C., Morand, C., Texier, O., Favier, M. L., Agullo, G., Demigné, C., Régérat, F., and Rémésy, C. (1995) *J. Nutr. 125*, 1911−1922.
28. Boulton, D. W., Walle, U. K., and Walle, T. (1998) *J. Pharm. Pharmacol. 50*, 243−249.
29. Reyftmann, J.-P., Morlière, P., Goldstein, S., Santus, R., Dubertret, L., and Lagrange, D. (1984) *Photochem. Photobiol. 40*, 721−729.
30. Candide, C., Morlière, P., Mazière, J.-C., Goldstein, S., Santus, R., Dubertret, L., Reyftmann, J.-P., and Polonovski, J. (1986) *FEBS Lett. 207*, 133−138.
31. Willson, R. L., Dunster, C. A., Forni, L. G., Gee, C. A., and Kittridge, K. J. (1985) *Philos. Trans. R. Soc. London, Ser. B 311*, 545−563.
32. Jovanovic, S. V., Steenken, S., Tosic, M., Marjanovic, B, and Simic, M. G. (1994) *J. Am. Chem. Soc. 116*, 4846−4851.
33. Jovanovic, S. V., Steenken, S., Simic, M. G., and Hara, Y. (1998) Antioxidant properties of flavonoids: reduction potential and electronic transfer reactions of flavonoid radicals, in *Flavonoids in Health and Disease* (Rice-Evans, C., and Packer, L., Eds.) pp 137−161, Marcel Dekker, New York.
34. Ames, B. N., Cathcart, R., Schwiers, E., and Hochstein, P. (1981) *Proc. Natl. Acad. Sci. U.S.A. 78*, 6858−6862.
35. Filipe, P., Lança, V., Silva, J. N., Morlière, P., Santus, R., and Fernandes, A. (2001) *Mol. Cell. Biochem. 221*, 79−87.
36. Santus, R., Patterson, L. K., Hug, G. L., Bazin, M., Mazière, J.-C., and Morlière, P. (2000) *Free Radical Res. 33*, 383−391.

BI026133+